

Synthesis and Characterization of Lithium Manganese Oxide (LiMn₂O₄) from Manganese Ore *via* Solid State Reaction Route

Sajjad Ali^a, Salar Ahmad^{b*}, Syed Ahmad Ali^a, Linta Khalid^a and Ikram Ullah^c

^aMaterials Research Laboratory, Department of Physics, University of Peshawar, Peshawar-25120, KPK, Pakistan

^bDepartment of Physics, Government Post Graduate College Timergara, Lower Dir-18300, KPK, Pakistan

^cDepartment of Natural Sciences and Humanities, University of Engineering and Technology, Mardan-23200, KPK, Pakistan

(received August 23, 2022; revised October 26, 2022; accepted October 31, 2022)

Abstract. Utilization of natural ores and extraction of valuable metals is an important and interesting research area. It is based on the current study which focuses on the solid-state reaction based synthesis of lithium manganese oxide (LiMn₂O₄) from Mn-Ore. From the Mn-Ore, manganese oxide (Mn₃O₄) was extracted and the powdered manganese oxide (Mn₃O₄) was then combined with lithium hydroxide monohydrate (LiOH·H₂O) to produce lithium manganese oxide (LiMn₂O₄). X-ray diffraction (XRD) analysis confirmed the formation of single phase lithium manganese oxide (LiMn₂O₄) with particle size 15.88 nm. Microstructural analysis shows a porous surface and confirms the formation of lithium manganese oxide (LiMn₂O₄) nanoparticles. Additionally, it demonstrates that the produced nanoparticles form and develop in a very synchronized manner. Elemental analysis of the samples further confirmed the successful synthesis of lithium manganese oxide (LiMn₂O₄) nanoparticles. Due to its simplicity and affordability, this process could be employed to develop lithium manganese oxide (LiMn₂O₄).

Keywords: solid state reaction route, lithium manganese oxide, nanoparticles, Mn-Ore

Introduction

The common alkali metals were found in plant matter, lithium was found in a mineral. This is said to explain how the word "lithos" which is Greek for "stone" came to be the name of the element. The least dense of all metals, lithium is a delicate, silvery metal. Due to its low density (0.534 g/cm³), high specific capacity (3860 mAh/gL) and low redox potential (3.04 V), lithium has outstanding physical properties. Another application for lithium is as a battery anode.

Harris looked at lithium's solubility in aqueous electrolytes. Most of the lithium is now produced from brines that, when combined with sodium carbonate, produce lithium carbonate. The fact that there is a direct chemical reaction between lithium and the electrolyte while still allowing for ionic transport across it incited studies on the stability of lithium ion batteries. Non-aqueous 3V lithium ion batteries and lithium sulphur dioxide were both commercially accessible in the 1960s, while lithium-manganese oxide (LiMnO₂) batteries were first made commercially available by the Sanyo firm, these batteries were first made available by Matsushita. Rechargeable lithium ion batteries were created because of improve-

ments in our understanding of the intercalation of lithium in various materials (Sreevaram *et al.*, 2016).

Due to the need for alchemists and glassmakers to distinguish between magnesia Negra (the black ore) and magnesia alba, manganese dioxide was likely referred to as manganesum in the 16th century (notice the two Ns instead of one) (a white ore, also from magnesia, also useful in glassmaking). Since the stone age, several vibrant manganese oxides have been employed as pigments. One such oxide is manganese dioxide, which is widely present in nature. Manganese was employed in the manufacture of steel around the turn of the 19th century and various patents were issued. With the invention of the Le-clanche cell in 1866 and the advancement of batteries employing manganese dioxide as a cathodic depolarizer, the demand for manganese dioxide soared. Most batteries contained manganese before nickel cadmium and lithium ion batteries were developed. Industrially generated manganese dioxide is typically used in batteries made of zinc, carbon since naturally occurring manganese dioxide includes impurities (Alessio *et al.*, 2007).

Due to their endurance, environmental compatibility and low cost, manganese oxides are utilized in a variety of industries like the production of dry cell batteries,

*Author for correspondence;

E-mail: ahmadsalar430@gmail.com

steel, colour, dyes, medicines, fertilisers and chemicals (Ngida *et al.*, 2019; Salehi, 2017). The extraction of manganese from its natural ores is a significant area of research because of its widespread application. Minerals containing manganese oxide have been utilised for centuries as colours and glass clarifying agents. Mn is employed as a metal, catalyst and battery component today. In a range of geological environments, more than 30 minerals of manganese oxide can be found. They are important parts of the Mn nodules that cover vast swaths of the ocean floor and many freshwater lake bottoms. Minerals of manganese oxide are widely distributed in sediments and soil and take part in several chemical processes that have an impact on groundwater and the overall composition of soil. It is challenging to investigate chemistries of crystals and their atomic structures because they typically appear as fine grained mixes (Bourg *et al.*, 2017).

The average concentration of manganese (Mn) in crustal rocks is 0.1%, it is the second most common heavy metal, after iron and the tenth most prevalent element in the Earth's crust. Mn has the same geochemical behaviour as Mg, Fe, Ni and Co and has a propensity to divide into minerals which appear during the initial stages of magmatic crystallisation. However, substantial amounts of Mn continue to exist in melts and can be found in large quantities in late-stage deposits like pegmatites. By interacting with groundwater and surface water, igneous and metamorphic rocks readily deplete Mn, which is also highly mobile in acidic aquatic systems as Mn (II) (London *et al.*, 2018).

Mn is quickly oxidised close to the surface of the earth, producing more than 30 different minerals of manganese oxide/hydroxide. These oxides are the main characters in the geochemistry and mineralogy of Mn in the upper crust as well as the main sources of Mn for industrial use. Many academics have already studied ways for economically extracting manganese oxides. Manganese does not naturally occur as a free element, instead, it is found in minerals along with iron and other elements. Mn oxides readily take part in exchange processes of cations and in a wide range of oxidation reduction processes in soils and sediments. They have substantial surface areas and have high chemical activity. Manganese has two oxidation states that it can exist in +2 and +3 and has the chemical formulas MnO and Mn₃O₄, respectively. When manganese is present in its purest form, it is more reactive. It is utilised in non-aqueous primary or secondary lithium batteries in addition to

aqueous primary or secondary alkaline batteries (Sun *et al.*, 2014).

Spinel made of lithium manganese oxide is extremely appealing for high power applications. Due to their three dimensional spinel structure, they have outstanding rate capability and provide higher safety characteristics than the nickel or cobalt system in the charged state. LiMn₂O₄ spinel has drawn a lot of interest due to its exceptional properties like as a catalyst in chemical reactions and as a cathode in lithium ion batteries (Deng *et al.*, 2004). High energy storage capability of lithium Mn-oxide as a cathode is widely recognised. The most suitable material to fabricate Li-Mn-O cathodes for batteries is Mn₃O₄ (Hong-zhe, 2010; Kurihara *et al.*, 2008). There are several ways to make Mn₃O₄, including solid state reactions, hydrothermal processes and low temperature reduction (Kurihara *et al.*, 2008). LiMn₂O₄ is one of the potential cathode materials for Li-ion batteries due to its non-toxic nature, accessibility and high open circuit voltage relative Li insertion. using a solid state reaction route. This process invariably produces Lithium manganese oxide with particles that are in the range of a nanoscale that can withstand high frequencies (Ahmad *et al.*, 2021).

In comparison to other synthesis methods, the solid-state reaction route takes less time. Additionally, ores like sulphide ore (if present) can be converted into oxides and will release as a gas when samples are heated without melting. A solid-state method for reaction route synthesis is typically less expensive and suitable for huge manufacturing. A molecule can be reduced.

Transition metal oxides, such as Mn-oxides are regarded as interesting materials for a variety of applications due to their good environmental compatibility, electrochemical properties and low cost (Ngida, 2020; Salehi, 2017; Sadek *et al.*, 2014; Dong, 2013). They are used in the production of steel, dry batteries, carbon zinc batteries, fertilisers, fine chemicals, colourants for brick and dyes and pharmaceuticals, among other industrial, technological and environmental uses. The efficient and economical extraction of Mn and Mn-oxides from low grade Mn-Ores has been the subject of numerous investigations. Manganese recovery techniques must be carried out in a reducing environment because Mn-Ores are stable in either an acidic or an alkaline oxidizing environment (Sinha *et al.*, 2019). The traditional extraction process uses coal as a reducing agent (Han *et al.*, 2015). However, this method involves a reaction that

occurs at a temperature more than 800 °C, which may have an impact on the reactor (Ismail *et al.*, 2004). Low grade manganese ores can be reduced recently by biomass cornstalk at a ratio of 10:3 at 500 °C, the manganese can then be extracted by vigorously swirling with 3 mol/L H₂SO₄ at 50 °C for 40 min, the yield was 90%. Additionally, molasses, methanol, lactose, sucrose and glucose are also well-known substances that leak in acidic environments (Furlani *et al.*, 2006). O₂ and Mn(OH)₂ combine gas solidically to form Mn₂O₃ nanoparticles (Mehdizadeh *et al.*, 2012; Davar, 2010). LiMn₂O₄ spinel has drawn a lot of interest due to its exceptional properties as its utilization in lithium ion batteries as a cathode and as a catalyst in chemical reactions (Sun *et al.*, 2014; Xu *et al.*, 2014). LiMn₂O₄ powder is commonly produced by mixing lithium salts, such as lithium hydroxide, carbonate or nitrate with manganese salts such as manganese oxide, hydroxide, or carbonate, at temperatures between 400 and 600 °C. The current project is centred on the Mn₃O₄ extraction from low grade Mn-Ore. The manganese oxides that are obtained are used to create nano LiMn₂O₄ (Brown *et al.*, 2012).

Experimental. For the synthesis of LiMn₂O₄, powder sample of Mn-Ore was weighted according to stoichiometric ratios using electronic analytical balance (KERN, ALS 220-4) and then sieved through a 100 mesh (74 µm size) (Brown *et al.*, 2012) in material research laboratory (MRL), Department of Physics University of Peshawar, Pakistan. For obtaining Mn₃O₄, 2.3 g of calcium carbonate was mixed with pure 3 g of Mn-Ore. To create a slurry, the obtained Mn₃O₄ powder (4 g) was mixed with 0.733 g of lithium hydroxide monohydrate (LiOH·H₂O). The combination was then processed for two hours in a horizontal ball mill using 1/4 diameter Y-hardened ZrO balls as milling medium and isopropanol as lubricants (Brown *et al.*, 2012). Furthermore, the sample was calcined at 750 °C for 3 h with temperature rise 5°/min using the Nabertherm LHT0₄/18 high temperature chamber furnace (1800 °C) at MRL, UOP (Ahmad *et al.*, 2021). The calcinated powders

Table 1. XRD specifications

Voltage	20-40 Kv
Current	2.3-3.0 A
X-ray	CuKα
Make	JDX-3532
Model	JDX-3532

were pressed into 2-3 mm high and 10 mm diameter pallets using 12 tonnes manual pallet press (CARVER, USA) at MRL (Brown *et al.*, 2012). X-ray diffractometer, installed in the centralized resources laboratory (CRL), university of Peshawar (UOP) was used for phase analysis of the sample. The specifications of the machine are given by Table 1.

SEM (scanning electron microscope) and EDX (energy dispersive X-ray) used to analyse the sample's microstructure and elemental composition, respectively. Table 2 provides the machine's specifications.

Results and Discussions

X-Ray Diffraction (XRD) analysis. Figure 1 shows the room temperature XRD graph of well-defined sharp diffraction peaks with low background indicating a good crystallinity. The 2θ values range from 10 to 70 as shown in Fig. 1. The sharp peak labelled as (a) in Fig. 4, at 37.302° is attributed to lithium manganese oxide phase (JCPDS 38-789). It confirmed the single phase of lithium manganese oxide with no other impurities or secondary phases. The small peaks labelled as (b) and (c) in Fig. 2, belong to the phase formation of Li₁₋₂MnO₂ (JCPDS 38-1282) and Mn₃O₄ (JCPDS 18-802) respectively.

Table 2. SEM specifications

Magnification	Upto 300,000X
Resolution	3.0 nm at 30kv
Make	JEOL, Japan
Model	Backscattered and secondary electron imaging
Coupled EDS	NCA 200/Oxford instruments, UK

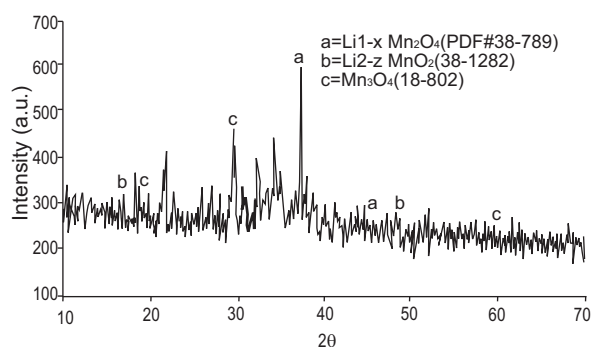


Fig. 1. X-ray diffraction (XRD) graph of the synthesized nanoparticles.

Table 3 lists the average crystallite size (D nm) values that were calculated using Scherrer formula equation 1. Table 3 show that the synthesized nanoparticles possess an average crystallite size of 15.88 nm which is in harmony with previously published experimental findings.

$$D = 0.89\lambda/\beta \cos\theta \dots\dots\dots (1)$$

where:

D is particle size, λ is wavelength of X-rays, β is the full width half maxima (FWHM) and θ is the corresponding diffraction angle.

Microstructural analysis. Figure 2 illustrates the results of a scanning electron microscope (SEM) investigation

Table 3. Crystallite size calculation of the synthesized nanoparticles

Peak position (2 theta)	FWHM	crystallite size D (nm)	D nm (average)
20.43267	25.54773	0.315968357	15.88328132
20.43267	0.7164	11.26783119	
24.62694	0.44744	18.17304413	
25.40753	0.31534	25.82496562	
27.96299	0.68691	11.91834986	
31.69799	0.47694	17.31502306	
36.84801	0.30284	27.64985773	
38.53789	0.27897	30.16718317	
42.26255	26.84136	0.317308753	

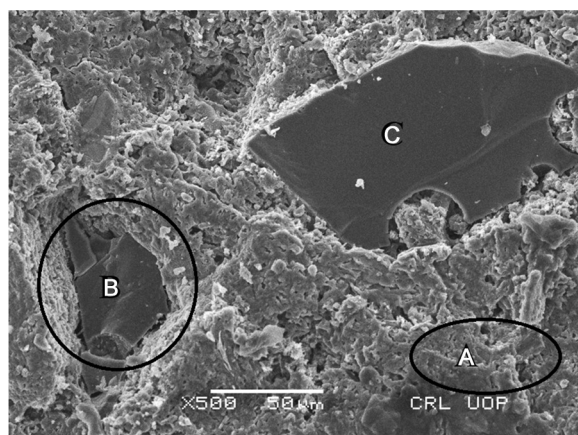


Fig. 2. Scanning electron microscope image of the synthesized lithium manganese oxide (LiMn₂O₄) nanoparticles showing different regions marked as (A, B and C).

of the materials' microstructure. Figure 2 shows many small pores on the surface which are produced due to the exhaust of gasses during thermal treatment of the samples (Ahmad *et al.*, 2021) found porous surface morphology and confirmed that it is due to incomplete solid to solid reactions. The nanoparticles are embedded in a thick silicate layer formed due to the presence of large amount of silica in Mn-Ore confirmed by the corresponding EDX spectra in Fig. 2 and Table 4. (Ahmad *et al.*, 2021) also found similar results and established that the nanoparticles are stacked in silicate layer. Lithium manganese oxide (LiMn₂O₄) nanoparticles labelled as (B) and (C) embedded in silicate layers possess an average particle size of 15.88 nm. The small white colour powder dispersed over the whole surface, specifically over region (c) which are Mn₃O₄ nanoparticles which were also reported in XRD analysis. Hence SEM analysis confirmed XRD analysis. Literature suggests that such type of surface morphology is responsible for best magnetic properties of the synthesized nanoparticles (Ahmad *et al.*, 2021). Elemental analysis of the micro-region (A) and (B) of Fig. 2 is given by Table 4.

Table. 4. Chemical composition of the micro regions in Fig. 2 labelled A, B, and C

Micro-region	O	Na	Mg	Al	Si	K	Ca	Mn
	(wt.%)							
Total	41.56	25.49	0.80	5.44	22.88	2.02	0.71	1.10
A	42.61	37.22	-	2.79	15.06	0.38	0.67	1.28
B	38.19	1.48	0.92	16.40	39.18	2.49	1.34	-
C	29.75	13.05	-	7.76	40.37	6.06	1.70	0.81

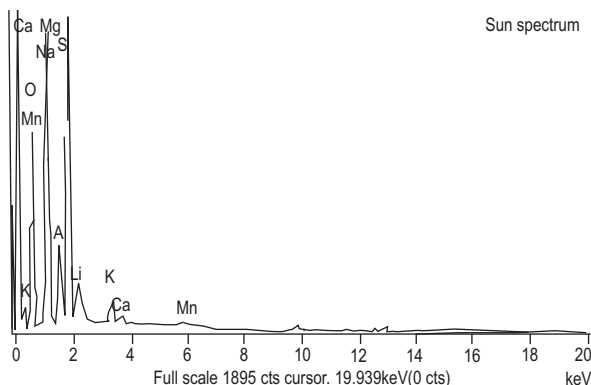


Fig. 3. Energy dispersive X-ray spectra of the synthesized samples.

EDX analysis. To confirm the formation of lithium manganese oxide, EDX analysis of the sample was performed as shown in Fig. 3. The weight percent and atomic weight percent of different elements is given in Table 5. The presence of oxygen and silicon confirm the formation of silicate layers which was reported in the SEM analysis. EDX spectra (Fig. 3) also confirmed the presence of 1.29 wt.% of lithium which accounts for the phase formation of Lithium manganese oxide (LiMn_2O_4). Similar phase was also reported by XRD-analysis hence EDX-analysis confirmed XRD-analysis. Table 5 shows the existence of high content O (42.61 wt.%) and Mn (1.28 wt.%). For more insight, the weight percent is also given by the pie chart in Fig. 4.

Table 5. Elemental concentrations (wt. %) of different elements

Element	Weight (%)	Atomic (%)
O	42.61	53.58
Na	35.93	32.56
Al	2.79	2.08
Si	15.06	10.78
K	0.38	0.20
Ca	0.67	0.33
Mn	1.28	0.47
Li	1.29	0.48
Total	100.00	

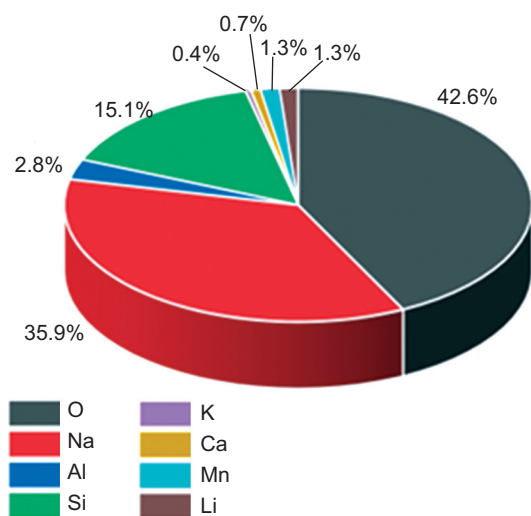


Fig. 4. Pie chart of the elements (by wt. %).

Conclusion

Lithium manganese oxide (LiMn_2O_4) has been successfully synthesized from manganese ore via solid state

reaction route which is less time consuming and highly economical synthesis technique. X-ray analysis revealed lithium manganese oxide nanoparticles with particle size in perfect agreement with previously published experimental findings. The presence of nanoparticles was further confirmed by scanning electron microscope. It has been established that the nanoparticles are embedded in silicate layers. These layers are formed due to huge amount of silica present in Mn-Ore which was used during the synthesis process. It has been determined that the synthesized sample include a trace amount of lithium which can be used in batteries and energy storage devices.

Conflict of Interest. The authors declare that they have no conflict of interest.

References

- Ahmad, S., Ali, S., Ullah, I., Zobaer, M.S., Albakri, A., Muhammad, T. 2021. Synthesis and characterization of manganese ferrite from low grade manganese ore through solid state reaction route. *Scientific Reports*, **11**: 1-9.
- Alessio, L., Campagna, M., Lucchini, R. 2007. From lead to manganese through mercury: mythology, science and lessons for prevention. *American Journal of Industrial Medicine*, **50**: 779-787.
- Bourg, I.C., Ajo-Franklin-Jonathan, B. 2017. Clay, water and salt: controls on the permeability of fine-grained sedimentary rocks. *Accounts of Chemical Research*, **50**: 2067-2074.
- Brown, J.G. 2012. *X-rays and Their Applications*, pp. 258, E-Book, Springer Science and Business Media.
- Davar, F., Salavati-Niasari, M., Mir, N., Saberyan, K., Monemzadeh, M., Ahmadi, E. 2010. Thermal decomposition route for synthesis of Mn_3O_4 nanoparticles in presence of a novel precursor. *Polyhedron*, **29**: 1747-1753.
- Deng, B., Nakamura, H., Zhang, Q., Yoshio, M., Xia, Y. 2004. Greatly improved elevated temperature cycling behaviour of $\text{Li}^{+1} \times \text{MgyMn}_{2-x-y}\text{O}_{4+\delta}$ spinels with controlled oxygen stoichiometry. *Electrochimica Acta*, **49**: 1823-1830.
- Dong, R., Ye, Q., Kuang, L., Lu, X., Zhang, Y., Zhang, X., Tan, G., Wen, Y., Wang, F. 2013. Enhanced supercapacitor performance of Mn_3O_4 nanocrystals by doping transition metal ions. *ACS Applied Materials and Interfaces*, **5**: 9508-9516.
- Furlani, G., Pagnanelli, F., Toro, L. 2006. Reductive

- acid leaching of manganese dioxide with glucose: identification of oxidation derivatives of glucose. *Hydrometallurgy*, **81**: 234-240.
- Han, H., Duan, D., Yuan, P., Li, D. 2015. Biomass reducing agent utilisation in rotary hearth furnace process for DRI production. *Ironmaking and Steel-making*, **42**: 579-584.
- Hong-zhe, W., Hui-ling, Z., Bing, L., Xing-tang, Z., Du Zu-liang, Wen-sheng, Y. 2010. Facile preparation of Mn₂O₃ nanowires by thermal decomposition of MnCO₃. *Chemical Research in Chinese Universities*, **26**: 5-7.
- Ismail, A.A., Ali, E.A., Ibrahim, I.A., Ahmed, M.S. 2004. A comparative study on acid leaching of low grade manganese ore using some industrial wastes as reductants. *The Canadian Journal of Chemical Engineering*, **82**: 1296-1300.
- Kurihara, H., Yajima, T., Suzuki, S. 2008. Preparation of cathode active material for rechargeable magnesium battery by atmospheric pressure microwave discharge using carbon felt pieces. *Chemistry Letters*, **37**: 376-377.
- London, D. 2018. Ore-forming processes within granitic pegmatites. *Ore Geology Reviews*, **101**: 349-383.
- Mehdizadeh, R., Saghatforoush, L.A., Sanati, S. 2012. Solvothermal synthesis and characterization of α -Fe₂O₃ nanodiscs and Mn₃O₄ nanoparticles with 1, 10-phenanthroline. *Superlattices and Microstructures*, **52**: 92-98.
- Ngida, R.E., Zawrah, M.F., Khattab, R.M., Heikal, E. 2019. Hydrothermal synthesis, sintering and characterization of nano La-manganite perovskite doped with Ca or Sr. *Ceramics International*, **45**: 4894-4901.
- Sadek, H.E.H., Khattab, R.M., Gaber, A.A., Zawrah, M.F. 2014. Nano Mg⁺¹ × NixAl₂O₄ spinel pigments for advanced applications. *Spectrochimica Acta Part A: Molecular and Biomolecular Spectroscopy*, **125**: 353-358.
- Salehi, M., Ghasemi, F. 2017. Novel synthesis of manganese spinely nanoparticles via combustion with Mn(III) (acac) 3 as precursor. *International Journal of Nanoscience and Nanotechnology*, **13**: 151-158.
- Sinha, M.K., Purcell, W. 2019. Reducing agents in the leaching of manganese ores: a comprehensive review. *Hydrometallurgy*, **187**: 168-186.
- Sreevaram, T., Kumar, N.V., Sailaja, B.B.V. 2016. Chemical speciation of binary complexes of Ca (II), Mg (II) and Zn (II) with Maleic acid in ethylene glycol-water mixtures. *Journal of Pharma Chemical Biological Science*, **3**: 543-552.
- Sun, Y., Xu, C., Li, B., Xu, J., He, Y., Du, H., Kang, F. 2014. Synthesis of single crystalline LiMn₂O₄ with different dimensional nanostructures for Li-ion batteries. *International Journal of Electrochemical Sciences*, **9**: 6387-6401.
- Xu, G.L., Wang, Q., Fang, J.C., Xu, Y.F., Li, J.T., Huang, L., Sun, S.G. 2014. Tuning the structure and property of nanostructured cathode materials of lithium ion and lithium sulfur batteries. *Journal of Materials Chemistry A*, **2**: 19941-19962.